J Mater Sci: Mater Electron (2021) 32:22579–22587

Crystal structure, physicochemical, and sensory properties of solid solutions $Bi_{1-x}La_xFe_{1-x}Co_xO_3$ (x = 0, 0.05, 0.1)

Anna Glinskaya[1,*], Gennady Petrov[1], and Valentin Romanovski[2,3]

[1] Belarusian State Technological University, Sverdlova, 13a, 220006 Minsk, Belarus
[2] Institute of General and Inorganic Chemistry, National Academy of Sciences of Belarus, Surganova 9/1, 220072 Minsk, Belarus
[3] Center of Functional Nano-Ceramics, National University of Science and Technology «MISIS», Lenin av., 4, Moscow, Russia 119049

Received: 19 February 2021
Accepted: 31 July 2021
Published online: 19 August 2021

ABSTRACT

For the first time, the synthesis was carried out and the physicochemical properties of solid solutions based on the multiferroic $BiFeO_3$ were studied. It was found that the samples were characterized by a rhombohedrally distorted perovskite structure. It was shown that a slight isovalent substitution of Bi^{3+} ions by La^{3+} ions and Fe^{3+} ions by Co^{3+} ions in $BiFeO_3$ ($x \leq 0.10$) leads to an increase in the specific magnetization. This can be attributed to structural distortions and causes weak ferromagnetism to occur. The studied samples are *p*-type semiconductors and have good sensory properties even without catalysts. It was found that the maximum values of the S response were obtained at temperatures close to the ferromagnetic Curie temperature, the value of which is consistent with the studies of electrical properties.

1 Introduction

State-of-art development of microelectronics requires creation of new materials with a wide range of physical properties. Over the recent years, there has been a continuing interest in the study of the physicochemical properties of multiferroics (ferroelectromagnets) based on bismuth ferrites ($BiFeO_3$, $Bi_2Fe_4O_9$, etc.) where ferromagnetism and ferroelectricity exist simultaneously. These compounds are thoroughly studied [1] because of their sensory [2–6], catalytic [7, 8], and other functional properties [9–12]. The connection between the magnetic and electrical subsystems in multiferroics makes it possible to control the magnetic properties of the material with the help of an electric field and vice versa, which makes it possible to create multiferroics-based devices with fundamentally new functionality. That is why multiferroics are considered as promising materials for sensor electronics, information processing and storage devices, spintronic devices, microwave technology, and many other applications.

The best studied ferroelectromagnet is $BiFeO_3$ with a perovskite structure, which is mostly due to the high temperatures of its magnetic (T_N = 643 K) and electrical ordering (T_C = 1083 K). This makes $BiFeO_3$

Address correspondence to E-mail: GlinskayaA@belstu.by

https://doi.org/10.1007/s10854-021-06743-3

a promising basic compound for new materials with high values of electric polarization and magnetization at room temperature. However, solid solutions based on this ferrite have been studied to a lesser extent, and the literature data suggest that even with an insignificant substitution of Bi^{3+} ions by Pr^{3+} ions [8, 13], Sm^{3+} and Mn^{3+}, Co^{3+}, Cr^{3+} [14], Y^{3+} and Sc^{3+} [15], La^{3+} [16], Gd^{3+} and Mn^{3+} [17], Sm^{3+} [18], La^{3+} and Mn^{3+} [19], etc., and Fe^{3+} ions by ferroactive Ti^{4+}, Nb^{5+} ions [20], the inhomogeneous spatially modulated spin structure of the cycloidal type is destroyed. Such structure is characteristic for this compound and does not show intense magnetoelectric properties. It should be noted that there is practically no information in the literature on $BiFeO_3$-based solid solutions, in which simultaneous isovalent replacement of Bi^{3+} ions by rare-earth ions and Fe^{3+} ions by paramagnetic 3d-metal ions would be carried out [21–23]. In the works [21–23] of the structure and magnetic properties of samples with insignificant substitution in the iron sublattice (up to 5%), for example, $(Bi_{0.9}La_{0.1})$ $(Fe_{0.95}Co_x)O_3$ (x = 0, 0.01, 0.05) [21], $Bi_{0.84}La_{0.1}6Fe_{1-x}Co_xO_3$ x = 0.02–0.1 [22], and $Bi_{0.9}La_{0.1}Fe_{0.97}Co_{0.03}O_3$ [23] were studied, but the sensory properties of materials are not considered. It is shown that such a substitution can contribute to the production of ferroelectric materials with improved properties, since in certain cases partial substitution of ions makes it possible to smoothly control physicochemical properties of the samples. In this work, we have investigated not only crystal structure, magnetic, and electrical properties but also sensory properties of $Bi_{1-x}La_xFe_{1-x}Co_xO_3$ solid solutions (x = 0.05; 0.1), formed at simultaneous substitution of Bi^{3+} ions by La^{3+} ions and Fe^{3+} ions by Co^{3+} ions in $BiFeO_3$.

2 Materials and methods

2.1 Materials and reagents

All oxides (Bi_2O_3, Fe_2O_3, La_2O_3, Co_3O_4) were of analytical grade (Merck). Contents of the basic substances in the above oxides were at least 99.99%.

2.2 Method of synthesis

Synthesis of polycrystalline samples $Bi_{1-x}La_xFe_{1-x}Co_xO_3$ ($0 \le x \le 0.10$) was carried out by solid-phase reactions from the corresponding oxides Bi_2O_3, Fe_2O_3, La_2O_3, and Co_3O_4. La_2O_3 oxide was calcined in air at a temperature of 1000 °C for 2 h. Powders of the starting materials taken in the set molar ratios were mixed and ground for 30 min in a planetary mill with the addition of ethanol. The resulting mixture was compressed under pressure of 50–75 MPa into tablets with 25 mm across diameter and 5–7 mm thickness. The tablets were then fired at 800 °C in air for 8 h. After that the tablets were crushed, grounded, and pressed into bars of 30 mm length and a section of 5 × 5 mm. $BiFeO_3$ sample was annealed in air at a temperature of 870 °C for 10 min. Samples with x = 0.05 and 0.10 were annealed in air at 950 °C for 8 h since the preparation of single-phase $BiFeO_3$ is difficult due to the complexity of the phase diagram of the Bi_2O_3–Fe_2O_3 system, which allows the formation of two other binary compounds, i.e., $Bi_2Fe_4O_9$ and $Bi_{25}FeO_{39}$.

2.3 Materials characterization

X-ray diffraction patterns were obtained on a D8 ADVANCED Bruker diffractometer using CuKα radiation. IR spectra were recorded in the wavenumber range of 350–900 cm^{-1} in mixtures pelleted with KBr on a NEXUS IR Fourier spectrometer (THERMO NICOLET) with an error of ± 2 cm^{-1}.

Sensory properties were determined using sintered thick film samples on ceramic substrates. Suspension of powdery solid solutions in ethanol was deposited on the ceramic plate. Further, the plate was dried in air at 373 K and then it was annealed in air at 1073 K for 2 h. Finally, the Ag contacts (suspension of powdery Ag in isoamyl acetate) were deposited on the edges of such a thick film structure. Ag wires were also used as electric conductors. Gas-sensitive element (layer) of the sensor made of bismuth ferrite usually had 5–7 mm width, 10–12 mm length. Its thickness did not exceed 0.5 mm. Silver paste and wire were used as contacts. The internal volume of the measuring cell was about 140 cm^3, and the cell was placed in a resistance tube furnace with a controlled temperature.

Electrical conductivity of the samples was measured in air in the temperature range of 300–1100 K by four-contact method. Silver contacts were also used.

Specific magnetization (σ_{sp}) of the samples was measured by the Faraday method in the temperature

range of 77–1000 K in the Scientific-Practical Materials Research Center of NAS of Belarus.

3 Results and discussion

The results of X-ray diffraction analysis made it possible to establish that the substitution of up to 10 mol% of Bi^{3+}, Fe^{3+} ions by La^{3+}, Co^{3+} ions in $BiFeO_3$ ferrite led to the formation of a continuous series of solid solutions (Fig. 1). This is evidenced by a gradual decrease in parameter a and an increase in the angle α of the crystal lattice of rhombohedrally distorted perovskite (Table 1).

The patterns of changes in the frequencies of absorption bands caused by stretching and deformation vibrations, depending on the degree of substitution x, are confirmed by the data of X-ray phase analysis. The broad absorption bands in the spectra in the region of $\approx$540–615 cm^{-1} characterize the vibrations of B–O bonds in the BO_6 octahedra of the ABO_3 perovskite. With an increase in the substitution degree, this absorption band was shifted to the high-frequency region. This is a consequence of a decrease in the B–O bond lengths (Fe^{3+}–O, Co^{3+}–O). In this case, the nature of the change in absorption frequencies caused by deformation vibrations changes insignificantly with an increase in the degree of substitution x and slightly shifts to the high-frequency region.

The distortion of the structure is due to the fact that the effective ionic radius of the trivalent bismuth ion Bi^{3+} ($r(Bi^{3+})$ = 1.20 Å) was greater than the effective ionic radius of La^{3+} ($r(La^{3+})$ = 1.04 Å) with the same anionic environment [24], and the effective ionic radii of the trivalent ions Fe^{3+} and Co^{3+} at the same anionic environment differ insignificantly and are $r(Fe^{3+})$ = 0.67 Å and $r(Co^{3+})$ = 0.64 Å [24], respectively. It should be noted that the studied samples contained an insignificant amount of impurity phases of ferrites $Bi_2Fe_4O_9$ and $Bi_{25}FeO_{39}$ which was recorded on electron microscopic images of chips of ceramic samples of the studied solid solutions (Fig. 2). Compositions of these grains ($Bi_{25}FeO_{39}$ and $Bi_2Fe_4O_9$) were assigned on the basis of the results of determination of Bi- and Fe-content by EDX results. Theoretical content of Bi and Fe in the $Bi_2Fe_4O_9$ was 53.22 and 28.44 wt%, respectively, while these values for the $Bi_{25}FeO_{39}$ were 88.49 and 0.95 wt%, respectively.

In addition, according to the results of X-ray phase analysis, the $Bi_{0.9}La_{0.1}Fe_{0.9}Co_{0.1}O_3$ sample also contained a certain amount of ferromagnetic cobalt ferrite phase $CoFe_2O_4$, Curie temperature (T_c), and specific saturation magnetization (σ_s) at T = 0 K for which were 793 K and 90 G·cm^3/g [25]. The presence of other impurity phases in the samples of solid solutions with the composition $Bi_{1-x}La_xFe_{1-x}Co_xO_3$ ($0.05 \le x \le 0.1$), including ferrite $LaFe_{11}{}^{3+}Fe^{2+}O_{19}$, for which T_c was 695 K, and σ_s at a temperature of T = 100 K was 17.5 μB (88 G·cm^3/g) [26], was not detected. The impossibility of obtaining $BiFeO_3$ without impurities of other compounds existing in the Bi_2O_3–Fe_2O_3 system by solid-state interaction of oxides of bismuth (III) and iron (III) is also evidenced by numerous literature data [27, 28]. According to a number of authors, the formation of impurity secondary phases $Bi_{25}FeO_{39}$, $Bi_2Fe_4O_9$ occurs independently of the synthesis method: solid-state ceramic method, sol–gel technology, and other methods. In the synthesis of $BiFeO_3$, the high volatility of Bi_2O_3 led to the formation of the $Bi_2Fe_4O_9$ phase with a

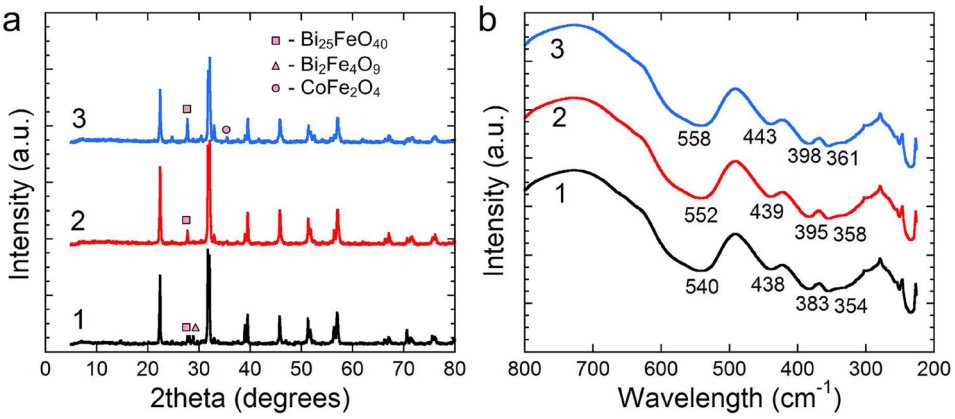

Fig. 1 X-ray diffraction patterns (**a**) and IR spectra (**b**) of samples $Bi_{1-x}La_xFe_{1-x}Co_xO_3$ at different values of x: 0 (*1*); 0.05 (*2*); 0.1 (*3*)

Table 1 Crystal lattice parameters of solid solutions of ferrite-cobaltites $Bi_{1-x}La_xFe_{1-x}Co_xO_3$ at different values of x

Substitution degree, x	a, Å	Angle α, degree	V, Å^3	Structure type
0	3.962 (2)	89.433	62.190	R ($R3c$)
0.05	3.961 (2)	89.474	62.117	R ($R3c$)
0.1	3.955 (2)	89.642	61.872	R ($R3c$)

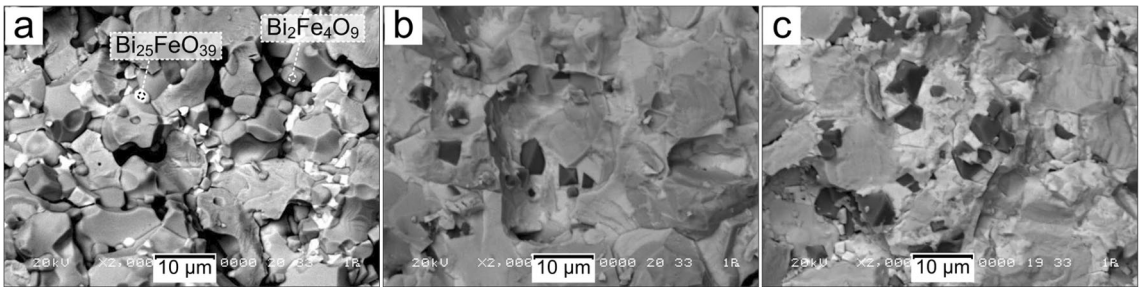

Fig. 2 SEM images of ceramic chips $BiFeO_3$ (**a**), $Bi_{0.95}La_{0.05}Fe_{0.95}Co_{0.05}O_3$ (**b**) and $Bi_{0.9}La_{0.1}Fe_{0.9}Co_{0.1}O_3$ (**c**)

lower bismuth content compared with $BiFeO_3$, while an insignificant excess of Bi_2O_3 in the reagent mixture led to the formation of the $Bi_{25}FeO_{39}$ phase with a higher bismuth content as compared to $BiFeO_3$. However, our earlier study of the magnetic properties of $Bi_{25}FeO_{39}$ and $Bi_2Fe_4O_9$ [29] made it possible to establish that these compounds do not contribute to the ferromagnetism of the resulting solid solutions based on bismuth ferrite $BiFeO_3$, since $Bi_{25}FeO_{39}$ exhibits paramagnetic properties in the temperature range of 5–1000 K, and $Bi_2Fe_4O_9$ is an antiferromagnet (with a Neel temperature T_N = 258 K) without signs of weak ferromagnetism. This was evidenced by the absence of magnetic hysteresis on the curves of the field dependence of magnetization [29]. This circumstance seems to be important since in some works [7] the presence of weak ferromagnetism in $BiFeO_3$ was associated namely with the presence of the impurity phase $Bi_{25}FeO_{39}$ which was considered a weak ferromagnet.

The results of measuring the electrical conductivity (σ) of ceramic samples $Bi_{1-x}La_xFe_{1-x}Co_xO_3$ in the range 300–1100 K (Fig. 3) showed that an increase in temperature led to an increase in electrical conductivity (σ), i.e., the samples are semiconductors. According to [30, 31], the solid solutions based on $BiFeO_3$ are semiconductors of the p-type.

In this case, an increase in the degree of substitution x of Bi^{3+} ions in $BiFeO_3$ by La^{3+} ions and Fe^{3+} ions by Co^{3+} ions led to a gradual increase in σ. The obtained dependences of E_A on T for the studied samples of ferrite-cobaltites pass through a maximum. The activation energy was maximum at temperature 670 K for a sample with a degree of substitution x = 0.05, and for a solid solution with x = 0.1 it rises to 740 K, which were close to the Curie temperature (T_c = 750 K) for the ferromagnetic phase of these samples. This was evidenced by the results of the magnetic properties of the samples (Fig. 4). At increase in the degree of substitution of diamagnetic Bi^{3+} ions by La^{3+} diamagnetic ions and Fe^{3+} paramagnetic ions by Co^{3+} ions (which at temperatures below 300 K are in a low-spin (LS) diamagnetic state, and at higher temperatures, in a paramagnetic intermediate (IS) or high-spin (HS) states), specific magnetization (σ_{sp}) gradually increases. Such an increase in σ_{sp} at increase in the degree of substitution x may be explained by structural distortion when Bi^{3+} ions in $BiFeO_3$ are substituted by rare-earth ions with a smaller ionic radius than bismuth ions [24]. This contributes to the destruction of the spiral spatially modulated structure of bismuth ferrite and the appearance of weak ferromagnetism [1]. Thus, at an increase in the degree of substitution x from 5 to 10 mol%, there was a gradual destruction of antiferromagnetic ordering and nucleation of ferromagnetic ordering in the samples where the Curie temperature changes insignificantly.

Sensory properties were assessed by the difference in electrical resistances of thick films measured in air (R_{air}) and in air containing a certain amount of vapors of the corresponding substances (R_{gas}): $S = (R_{gas}–R_{air})\cdot100\%/R_{air}$. The sensory properties of the obtained samples were investigated for the content of

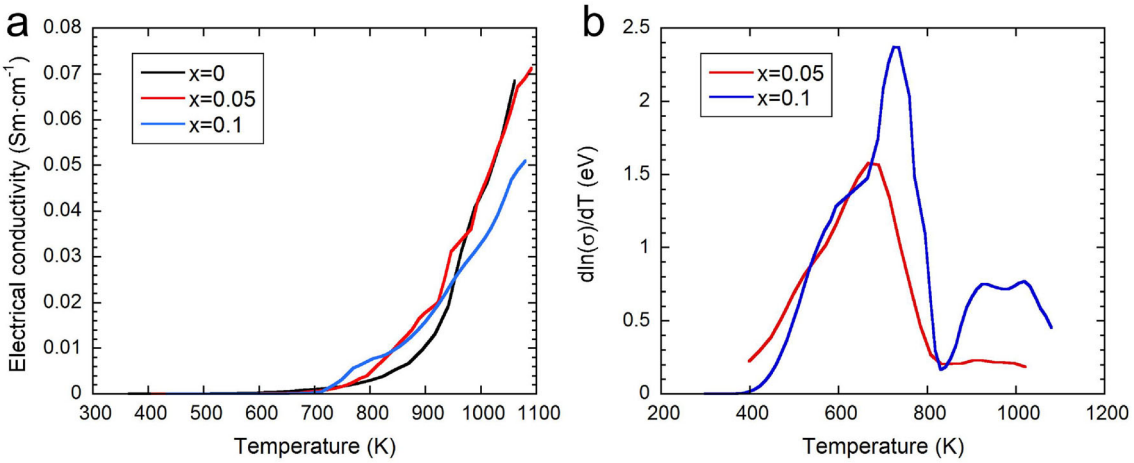

Fig. 3 Temperature dependence of **a** electrical conductivity (σ) and **b** derivative d$ln(\sigma)$/dT (of the activation energy E_A) of electrical conductivity for samples $Bi_{1-x}La_xFe_{1-x}Co_xO_3$ at different values of x

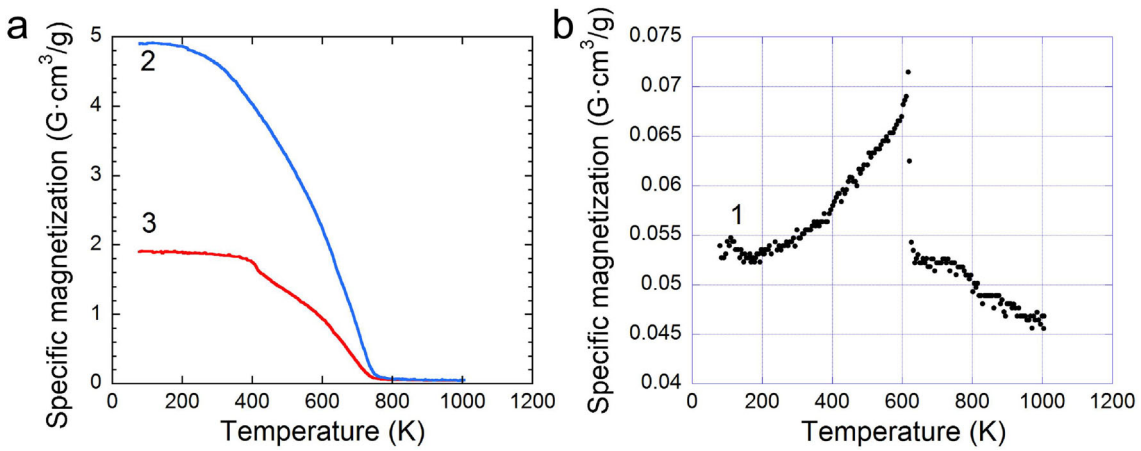

Fig. 4 Temperature dependences of specific magnetization (σ_{sp}) of samples 2 and 3 (**a**) and sample 1 (**b**) with varying degrees of substitution x: 0 (*1*); 0.05 (*2*); 0.1 (*3*)

ethanol, butanol, acetone, diethyl ether, AI-92 gasoline in the air.

Firstly, the temperatures of the maximum of response (S) values were determined. Typical example of the temperature dependence of the S for the $Bi_{0.9}La_{0.1}Fe_{0.9}Co_{0.1}O_3$ (at the fixed content of acetone in air) is given in Fig. 5.

For all the studied gases, these temperatures exceeded 250 °C (523 K) and depended on the nature of gas (being in the range of 677–780 K). Then, for temperatures corresponding to the maxima of S, the concentration dependences $S = f(C)$ were obtained, as shown in Fig. 6 (for the $Bi_{0.9}La_{0.1}Fe_{0.9}Co_{0.1}O_3$ sample with better sensory characteristics). As seen from Fig. 6, the sharpest increase in the S of the sample was observed at low gas concentrations. In the region of high vapor content in the air, the response of the sample tends to saturation. But, for diethyl ether, which has the lowest boiling point of the investigated gases, with a high content of its vapors in the air, ignition occurred when diethyl ether vapors were introduced into the measuring cell heated to the operating temperature. It is shown that the maximum values of S were obtained for the $Bi_{0.9}La_{0.1}Fe_{0.9}Co_{0.1}O_3$ sample at temperatures close to the ferromagnetic Curie temperature. The maximum values of the response S to vapors of various substances for samples with $x = 0.1$ varied from 200 to 750% (in the case of gasoline vapors) at vapor concentrations in the air up to 14,000 ppm. Films made of pure $BiFeO_3$ had the lowest gas sensitivity and the highest resistance.

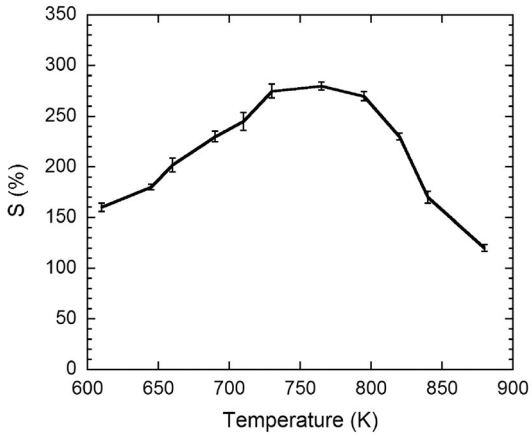

Fig. 5 Temperature dependence of the S value for $Bi_{0.9}La_{0.1}Fe_{0.9}Co_{0.1}O_3$ at the fixed content of acetone in air

Resistance (R_{air}) of the samples (*a–e*) in air (at the above temperatures) were 360 Ohm, 110 Ohm, 370 Ohm, 865 Ohm, and 580 Ohm, respectively. Note that difference in R_{air} values of the thick films in particular may be due to the difference in the dimension (length, width, thickness) of the films studied.

Table 2 compares some data on the study of the response (S) of a thick film based on undoped bismuth ferrite $BiFeO_3$ to the content of organic vapors in the air. The measurements were carried out at an operating temperature of 740 K. Results obtained for the $Bi_{0.9}La_{0.1}Fe_{0.9}Co_{0.1}O_3$ solid solution and undoped $BiFeO_3$ showed that the S values of the $BiFeO_3$-based sensor was noticeably lower compared to $Bi_{0.9}La_{0.1}Fe_{0.9}Co_{0.1}O_3$ solid solution. Thus, the partial isovalent substitution of simultaneous bismuth ions by lanthanum ions and iron ions by cobalt ions in the $BiFeO_3$ structure made it possible to significantly improve sensory properties of $BiFeO_3$. One of the reasons of the above increase of gas sensitivity of the solid solutions may be due to the catalytic properties of lanthanum and/or cobalt.

Important sensor characteristics are response time (for example, time to reach 90% signal value) and recovery time when the system is blowed by air. Generally, response and recovery times are highly dependent on the operating temperature of the sensor, the type of gas, and the volume of the measurement chamber. For all the gases studied by us for the

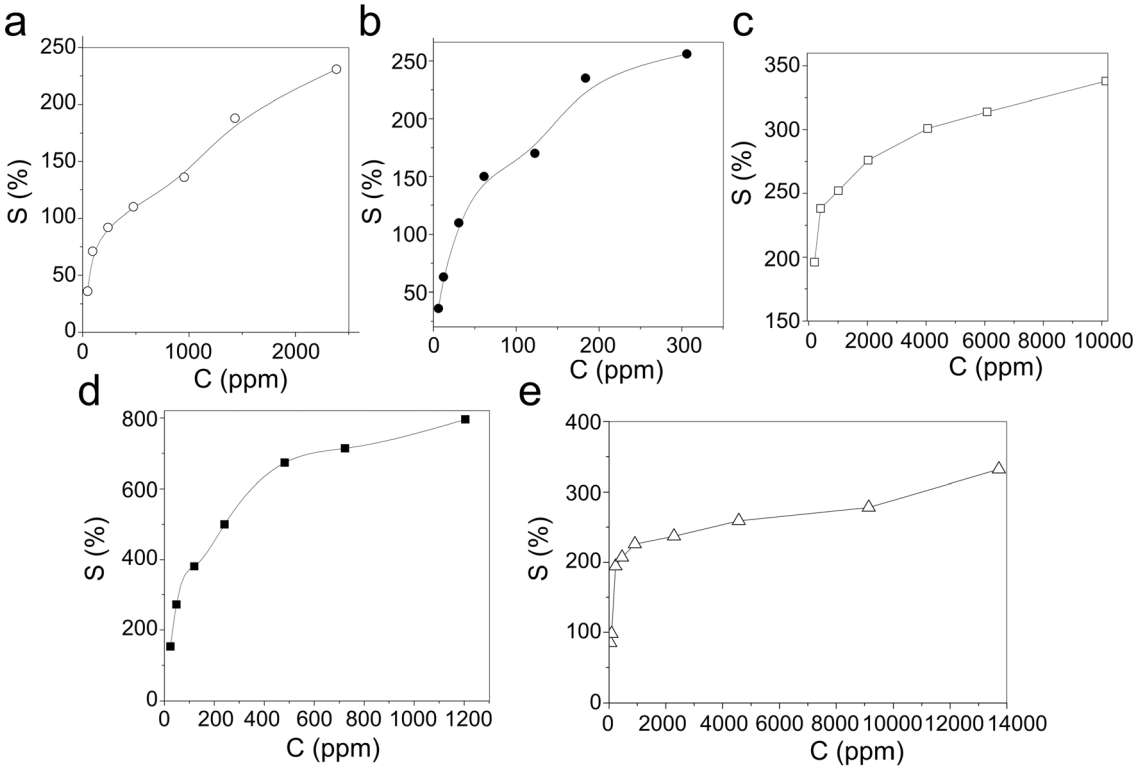

Fig. 6 Dependence of the magnitude of the response (S) of a thick film based on $Bi_{0.9}La_{0.1}Fe_{0.9}Co_{0.1}O_3$ on the concentration of vapors of various substances in the air: **a** ethanol ($T \approx 780\ K$); **b** butanol ($T \approx 775\ K$); **c** acetone ($T \approx 730\ K$); **d** petrol ($T \approx 705\ K$); **e** diethyl ether ($T \approx 677\ K$)

Table 2 Response values S of $BiFeO_3$ thick film

Substance	Ethanol	Butanol	Acetone	Diethyl ether	Petrol
Vapor concentration, C, ppm	2680	330	10,140	2300	1235
Response S, %	50	60	105	90	110

used thick film rather massive sensor with $x = 0.1$, these times mostly did not exceed 30 s. Probably, the miniaturization of the sensor (application of MEMS technologies with a built-in microheater) will somewhat reduce these times. Note that measurements of sensory properties were conducted with hand recording of the results (without automatic recording).

Since the investigated material was a p-type semiconductor, then, in the presence of reducing gases, as expected, its electrical resistance increased. For semiconductor gas sensors, the gas sensitivity mechanism is caused by a change in the surface resistance of the sensor during adsorption or desorption of oxygen. So, at low temperatures (below 250 °C [32] and according to other data below 100 °C [33]), oxygen molecules adsorbed on the sensor surface capture electrons from the valence band (conduction band) forming O_2^- ions [32]:

$$O_{2(gas)} + e \rightarrow O^-_{2(ads)}$$

At higher temperatures (above 250 °C) O_2^- particles dissociate into O^- and O^{2-} ions or these ions are formed according to the following scheme:

$$1/2O_{2(gas)} + e \rightarrow O^-_{(ads)}$$

$$1/2O_{2(gas)} + 2e \rightarrow O^{2-}_{(ads)}.$$

In this case, the concentration of electrons in the surface layer decreases, while the concentration of holes increases. The adsorbed oxygen ions oxidize the reducing gases. For example, for acetone the following oxidation schemes on p-type oxide semiconductors are usually proposed [33]:

$$CH_3COCH_3 + 8O^-_{(ads)} \rightarrow 3CO_2 + 3H_2O + 8e$$

$$CH_3COCH_3 + 6h^+ + 3O^{2-}_{(ads)} \rightarrow CH_3CHO + CO_2 + H_2O$$

$$CH_3CHO + 10h^+ + 5O^{2-}_{(ads)} \rightarrow 2CO_2 + 2H_2O.$$

Since the operating temperatures of the sensor exceeded 250 °C, the oxidation of the studied organic substances occurred due to the adsorbed O^- or O_2^- ions. It should be noted that the studied samples had good sensor properties even without catalysts (platinum or palladium). The introduction of catalysts can improve the sensory characteristics of such materials. Thus, sensors based on $Bi_{0.9}La_{0.1}Fe_{0.9}Co_{0.1}O_3$ can be installed in various industrial premises to detect perilous concentrations of vapors of the investigated combustible organic substances. The stability of the above sensors was tested and confirmed after keeping them in the air for one month. Difference of the S values before and after keeping of the samples in the most cases did not exceed ± 10%.

4 Conclusions

For the first time, the synthesis of solid solutions based on ferroelectric $BiFeO_3$ was carried out and their crystal structures, electrical, magnetic, and sensory properties were investigated. It was found that the samples obtained were characterized by a rhombohedrally distorted perovskite structure. The results of the studies of the magnetic properties showed that at a slight isovalent substitution of Bi^{3+} ions by La^{3+} ions and Fe^{3+} ions by Co^{3+} ions in $BiFeO_3$ ($0.05 \leq x \leq 0.10$), an increase in the specific magnetization occurs. This was a consequence of structural distortions due to the introduction of substituent ions into crystal structure of bismuth ferrite, which contributes to the destruction of the spiral spatially modulated structure of $BiFeO_3$ and the appearance of weak ferromagnetism. The data obtained on the temperature dependence of activation energy of electrical conductivity for the studied samples are in good consistence with the data of magnetic studies. It was shown that the temperature at which the value of the activation energy of electrical conductivity was maximum for samples with the degree of substitution $x = 0.05$ and 0.1 was close to the Curie temperature ($T_c = 750$ K) of the ferromagnetic phase of these samples. The study of the gas sensitivity of the materials made it possible to establish that the studied samples have good sensory properties even without catalysts (platinum or

palladium). It was shown that the maximum values of response *S* were obtained at temperatures close to the ferromagnetic Curie temperature, which is also consistent with other studies of the $Bi_{0.9}La_{0.1}Fe_{0.9}Co_{0.1}O_3$-based samples. Sensors can be installed in various industrial premises to detect perilous concentrations of vapors of the investigated combustible organic substances in the air.

Acknowledgements

The authors gratefully acknowledge the financial support of the Belarusian Republican Foundation for Basic Research (Project No. X18-PA017) and of the Ministry of Science and Higher Education of the Russian Federation in the framework of Increase Competitiveness Program of NUST «MISiS» (No. K2-2020-024), implemented by a governmental decree dated 16th of March 2013, N 211. Authors also acknowledge Dr. N.N. Lubinskii for help at investigation of sensory properties.

Author contributions

AG: Conceptualization, Methodology, Investigation, Visualization, Data curation, Writing original draft, and Review and Editing. GP: Investigation, Formal analysis, Data Curation, and Review. VR: Visualization, Data curation, Formal analysis, Writing—Original draft, and Writing—Review and Editing.

Declarations

Conflict of interest The authors declare that they have no competing interests.

References

1. G. Catalan, J.F. Scott, Adv. Mater. **21**(24), 2463 (2009). https://doi.org/10.1002/adma.200802849
2. S.D. Waghmare, S.D. Raut, B.G. Ghule, V.V. Jadhav, S.F. Shaikh, A.M. Al-Enizi, M. Ubaidullah, A. Nafady, B.M. Thamer, R.S. Mane, J. King Saud Univ. Sci. **32**, 3125 (2020). https://doi.org/10.1016/j.jksus.2020.08.024
3. X.L. Yu, Y. Wang, Y.M. Hu, C.B. Cao, H.L.W. Chan, J. Am. Ceram. Soc. **92**(12), 3105 (2009). https://doi.org/10.1111/j.1551-2916.2009.03325.x
4. P.A. Ghadage, U.R. Ghodake, J.Y. Patil, S.S. Suryavanshi, I.O.P. Conf, IOP Conf. Ser. Mater. Sci. Eng. **360**, 012063 (2018). https://doi.org/10.1088/1757-899X/360/1/012063
5. S. Mohamed Manjoor Shaib Maricar, D. Sastikumar, P. Reddy Vanga, M. Ashok, Mater. Today Proc. **39**(1), 245 (2021). https://doi.org/10.1016/j.matpr.2020.07.038
6. M. Patel, C. Mathai, N. Joshi, R. Jadhav, R. Pinto, IOSR J. Electr. Electron. Eng. Ver. I **10**, 2278 (2015). https://doi.org/10.9790/1676-10514547
7. Q. Zhang, W. Gong, J. Wang, X. Ning, Z. Wang, X. Zhao, W. Ren, Z. Zhang, J. Phys. Chem. C **115**, 25241 (2011). https://doi.org/10.1021/jp208750n
8. A. Haruna, S. Abdulkadir, O. Idris, Heliyon **6**(1), e03237-e3241 (2020). https://doi.org/10.1016/j.heliyon.2020.e03237
9. P. Uniyal, K.L. Yadav, J. Phys. Condens. Matter **21**(40), 405901 (2009). https://doi.org/10.1088/0953-8984/21/40/405901
10. L. Wu, C. Dong, H. Chen, J. Yao, C. Jiang, D. Xue, J. Am. Ceram. Soc. **95**(12), 3922 (2012). https://doi.org/10.1111/j.1551-2916.2012.05419.x
11. J.T. Han, Y.H. Huang, X.J. Wu, C.L. Wu, W. Wei, B. Peng, W. Huang, J.B. Goodenough, Adv. Mater. **18**(16), 2145 (2006). https://doi.org/10.1002/adma.200600072
12. J. Lu, A. Günther, F. Schrettle, F. Mayr, S. Krohns, P. Lunkenheimer, A. Pimenov, V.D. Travkin, A.A. Mukhin, A. Loidl, Eur. Phys. J. B **75**(4), 451 (2010). https://doi.org/10.1140/epjb/e2010-00170-x
13. V. Verma, A. Beniwal, A. Ohlan, R. Tripathi, J. Magn. Magn. Mater. **394**, 385 (2015). https://doi.org/10.1016/j.jmmm.2015.06.067
14. V. Verma, J. Alloys Compd. **641**, 205 (2015). https://doi.org/10.1016/j.jallcom.2015.03.260
15. A.K. Jena, J. Mohanty, J. Mater. Sci. Mater. Electron. **29**(6), 5150 (2018). https://doi.org/10.1007/s10854-017-8479-9
16. Z.X. Cheng, A.H. Li, X.L. Wang, S.X. Dou, K. Ozawa, H. Kimura, S.J. Zhang, T.R. Shrout, J. Appl. Phys. **103**(7), 07E507 (2008). https://doi.org/10.1063/1.2839325
17. P. Tang, D. Kuang, S. Yang, Y. Zhang, J. Alloys Compd. **656**, 912 (2016). https://doi.org/10.1016/j.jallcom.2015.10.010
18. K.S. Nalwa, A. Garg, J. Appl. Phys. **103**(4), 044101 (2008). https://doi.org/10.1063/1.2838483
19. V.R. Palkar, D.C. Kundaliya, S.K. Malik, J. Appl. Phys. **93**(7), 4337 (2003). https://doi.org/10.1063/1.1558992
20. M. Kumar, K.L. Yadav, J. Appl. Phys. **100**(7), 074111 (2006). https://doi.org/10.1063/1.2349491
21. Y. Gu, J. Zhao, W. Zhang, S. Liu, S. Ge, W. Chen, Y. Zhang, Ceram. Int. **42**(7), 8863 (2016). https://doi.org/10.1016/j.ceramint.2016.02.134
22. T.H. Le, N.V. Hao, N.H. Thoan, N.T.M. Hong, P.V. Hai, N.V. Thang, P.D. Thang, L.V. Nam, P.T. Tho, N.V. Dang, X.C.

Nguyen, Ceram. Int. **45**(15), 18480 (2019). https://doi.org/10.1016/j.ceramint.2019.06.066

23. Q.Q. Wang, C.C. Wang, N. Zhang, H. Wang, Y.D. Li, Q.J. Li, S.G. Huang, Y. Yu, Y.M. Guo, Z.Q. Lin, J. Alloys Compd. **745**, 401 (2018). https://doi.org/10.1016/j.jallcom.2018.02.014
24. M.P. Shaskolskaia, Crystallography (High School, Moscow, 1984) p. 376 (in Russian) http://www.geokniga.org/books/2904. Accessed 24 July 2020.
25. Y. Smith, H. Wayne, Ferrites (Instructor Lit., Moscow, 1962) p. 504 (in Russian) http://www.geokniga.org/bookfiles/geokniga-kristallografiya-shaskolskaya.djvu. Accessed 24 July 2020.
26. A. Aharoni, M. Schieber, Phys. Rev. **123**(3), 807 (1961). https://doi.org/10.1103/PhysRev.123.807
27. R. Palai, R.S. Katiyar, H. Schmid, P. Tissot, S.J. Clark, J. Robertson, S.A.T. Redfern, J.F. Scott, Phys. Rev. B (2007). https://doi.org/10.1103/PhysRevB.77.014110
28. G.D. Achenbach, W.J. James, R. Gerson, J. Am. Ceram. Soc. **50**(8), 437 (1967). https://doi.org/10.1111/j.1151-2916.1967.tb15153.x
29. A.A. Zatsiupa, L.A. Bashkirov, I.O. Troyanchuk, G.S. Petrov, A.I. Galyas, L.S. Lobanovski, S.V. Trukhanov, I.M. Sirota, Inorg. Mater. **49**(6), 616 (2013). https://doi.org/10.1134/S0020168513060204
30. Q. Xu, M. Sobhan, Q. Yang, F. Anariba, K.P. Ong, P. Wu, Dalton Trans. **43**(28), 10787 (2014). https://doi.org/10.1039/c4dt00468j
31. M. Schrade, N. Masó, A. Perejón, L.A. Pérez-Maqueda, A.R. West, J. Mater. Chem. C **38**, 10077 (2017). https://doi.org/10.1039/c7tc03345a
32. Y.J. Jeong, C. Balamurugan, D.W. Lee, Sens. Actuators B **229**, 288 (2016). https://doi.org/10.1134/S0020168513060204
33. B. Behera, S. Chandra, Sens. Actuators B **229**, 414 (2016). https://doi.org/10.1016/j.snb.2016.01.079